Radiation Exchange in Large Space Structures and Frames

A. F. Emery,* H. R. Mortazavi,? and M. N. Nguyen‡
University of Washington, Seattle, Washington

The computation of radiation view factors for curved surfaces is usually done by representing these surfaces by an assemblage of flat planes. For cylinders whose length-to-diameter ratio is large, such an approach may lead to inaccurate results because of the unfavorable aspect ratio of the planes. In addition, not only does this method require considerable computational effort, but when applied to sparse structures, such as those of space frames or fibrous insulation, may render the computations impractical, particularly if obstructed views are to be considered. This paper describes a special one-dimensional element which can be used in such circumstances. The basis of the element and its applications are described and several illustrative examples are presented.

Introduction

THE analysis of diffuse radiation heat transfer, whether between black surfaces or through absorbing media, is dominated by the need to determine the geometrical quantity, F_{ij}

$$A_i F_{ij} = \int\int \frac{e^{-kr_{ij}} \cos\theta_i \cos\theta_j}{\pi r_{ij}^2} dA_i dA_j \tag{1}$$

which is commonly called the view factor or shape factor, and which represents the fraction of diffuse radiative energy leaving surface i which strikes surface j. As expressed in the form of Eq. (1), the term e^{-kr} is used to account for the attenuation of the radiation as it passes through an absorbing medium with an extinction coefficient k. Although Eq. (1) is strictly correct only under limited conditions regarding the nature of the radiating surfaces and the absorbing medium,[1] the complexities of the solution of the general integro-differential equation of radiant transfer[2] are such that almost all engineering analyses are based upon the use of Eq. (1) or comparable simplifications.[3] For radiation through gases, the extinction coefficient k is generally wavelength dependent and a band model is commonly used with

$$Q_{ij} = \Sigma E_i(\lambda_1, \lambda_2) A_i F_{ij}(\lambda_1, \lambda_2) \tag{2}$$

$$A_i F_{ij}(\lambda_1, \lambda_2) = \int\int \frac{e^{-\bar{k}_{12} r_{ij}} \cos\theta_i \cos\theta_j}{\pi r_{ij}^2} dA_i dA_j \tag{3}$$

where $E(\lambda_1, \lambda_2)$ is the energy contained between wavelengths λ_1 and λ_2, and $\bar{k}_{12}$ represents an average extinction coefficient over the same wavelength range. Inasmuch as the spectrum may be divided into an arbitrary number of bands, it is important that the integrals in Eqs. (1) and (3) be evaluated accurately and efficiently, even if the surfaces have an obstructed view of each other. Although tables of view factors for a variety of relatively complex surface shapes exist,[4] evaluation of F_{ij} for structures of the type shown in Fig. 1 or for radiation through fibrous insulation with randomly oriented fibers as shown in Fig. 2 is not currently feasible.

Emery and co-workers[5-7] have described a numerical method based upon a combination of contour and double-area integration techniques for the rapid determination of F_{ij} for obstructed views. In this method, two surfaces, i and j, are subdivided into smaller subsurfaces or elemental areas. (In this paper, these elemental areas will be referred to as "elements.") The view factor is then computed by

$$A_i F_{ij} = \sum_{n}^{N} \sum_{m}^{M} A_n f_{nm} \phi_{nm} \tag{4}$$

where N and M are the number of elements for surfaces i and j, respectively, f_{nm} the view factor between the elements of the two surfaces, and ϕ_{nm} assumes the values of 1 or 0 depending on whether element n can see element m or not.

Thus, the problem has been expanded in difficulty, because now a total of NM elemental view factors must be determined, instead of one as before, and also the question of an obstructed view must be solved. Reference 5 contains a complete description of the method with emphasis on the evaluation of the obstruction function ϕ_{nm}. Reference 7 demonstrates the use of the method for the computation of radiation in the presence of an absorbing medium. In short, the method depends upon drawing a ray from the centroid of element n to the centroid of element m. Of all surfaces, those which are located between these two centroids are tested to see whether they obstruct the ray or not. Although conceptually simple, the efficient numerical implementation of this obstruction calculation requires certain assumptions which strongly influence the accuracy of the calculations, both of ϕ_{nm} and f_{nm}. It is assumed that 1) each surface is flat, and 2) each surface is bounded by no more than four sides.

Figures 3 and 4 illustrate the form of the computations. The calculation is based on subdividing each surface into small elements—which can be done efficiently only for three- or four-sided surfaces and even for four sides requires considerable care to yield elements of approximately equal areas. If the areas are too disparate, substantial errors are found in F_{ij}.[5] After the subdivision, it is determined if elements n and m face each other by drawing a ray from element n to m and comparing the direction of this ray with the surface normals N_n and N_m. If the elements do not face each other, ϕ_{nm} is set to zero; if they do face each other, then the obstruction function must be determined. This is done by first defining the minimum rectangular prism which contains surfaces i and j and excluding from further consideration all surfaces that do not penetrate this volume. This elimination procedure, which is comparable to the "clipping" operation in graphics, can only be done efficiently in rectangular coor-

Presented as Paper 83-1462 at the AIAA 18th Thermophysics Conference, Montreal, Canada, June 1-3, 1983; received June 20, 1983; revision received July 30, 1984. This paper is declared a work of the U.S. Government and therefore is in the public domain.

§Professor, Department of Mechanical Engineering.
†Ph.D. Candidate, Department of Mechanical Engineering.
‡Graduate Student, Department of Mechanical Engineering.

dinates and requires that the coordinates be transformed such that the line from the centroid of surface i to surface j be parallel to the z axis. Because these rotations must be done for every pair of surfaces, they require the continual redefinition of the corner coordinates. This clipping is also assisted materially if the surfaces have no more than four sides or corners. Each ray from surface i to surface j, i.e., from element n to element m, is examined for its intersection with possible obstructing surface **O.** If the surface is flat, this can be easily done by first finding the point of intersection with the infinite plane containing surface **O.** Finally, it is determined if the intersection point is within the edges of surface **O.** If so, $\phi_{nm}=0$, otherwise, $\phi_{nm}=1$ and the elements can see each other. Since the obstruction calculations are the most time-consuming part of the computation, it is best if the ray obstruction is detected early in the search of possible obstructing surfaces, implying the need for an ordering algorithm. However, testing of a variety of such ordering schemes has not proven effective and, in fact, it appears that the ordering is as time consuming as the direct evaluation of ϕ_{nm}.

The need to describe arbitrary surfaces by an assemblage of flat planes, of no more than four corners, imposes rather severe restrictions on the representation of such arbitrary surfaces and usually leads to the use of an unacceptably high number of such flat surfaces. This is particularly true for cylinders, for which at least eight or more flat surfaces are needed to yield acceptable results, Fig. 5. This point will be discussed further in a later section of this paper.

Most thermal analyzers contain one-dimensional conduction and convection elements. Such elements are often used to connect two thermal nodes without the need to construct a connecting two- or three-dimensional element and are defined in terms of the distance between the nodes and the effective thermal resistance. Similarly one-dimensional convection elements are used to represent fins or surface convectors by describing the product of the convection coefficient and the convecting area. Both elements are usually portrayed as cylindrical rods whose lengths, diameters, and thermal properties are adjusted to yield the correct thermal behavior. The space frame of Fig. 1 is typical of the structure that would be analyzed by such one-dimensional elements.

The comparable radiation element, a cylinder, while appearing to be similar at first, is not at all comparable. The orientation and shape of the conduction and convection elements are completely arbitrary as long as the elements possess the correct thermal characteristics. On the other hand, since radiation is dependent upon the precise surface shape, the one-dimensional radiation elements will have different view factors for different assumed shapes.

If a rod is taken to be the equivalent one-dimensional radiation element, the need to express its lateral surface as an assemblage of eight or more flat planes will, in the case of several such elements, lead to an extremely large number of surfaces with totally unacceptable computational times, especially for obstruction calculations.

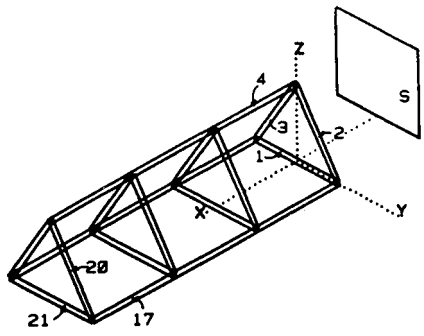

Fig. 1 Radiation from surface S to the members of a typical space structure (width of S and truss = 10; height of S = 10, truss = 8.66; length of truss = 30; location of S at $x=-15$).

In this paper, we first describe the use of flat planes to model cylinders and determine the minimum number of planes needed. The concept of the one-dimensional radiation element is introduced and it is shown how it can be modeled by a simple rotating quadrilateral. We illustrate the usefulness of this one-dimensional element, demonstrate its accuracy, and, finally, present several typical examples of its use in computing view factors for complex space structures and in determining an effective extinction coefficient for a random array of small fibers.

Modeling Circles and Cylinders

Before developing the one-dimensional radiation element, it is of interest to determine the degree of surface refinement needed to model curved surfaces or nonstraight boundaries. If, for example, cylinders can be modeled with a few elements, it is of little value to develop the special one-dimensional elements. On the other hand, if a large number of flat surfaces is needed, then it is important to develop this element and demonstrate its accuracy.

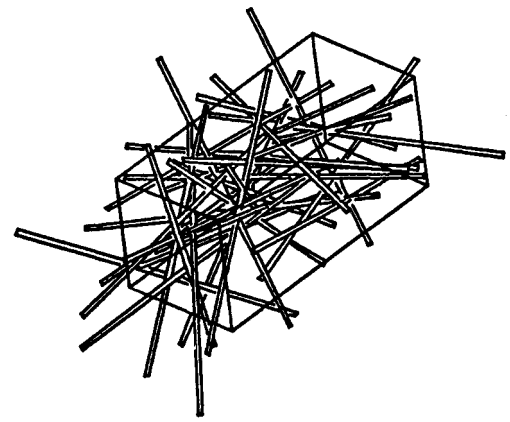

Fig. 2 Schematic representation of a fibrous insulation.

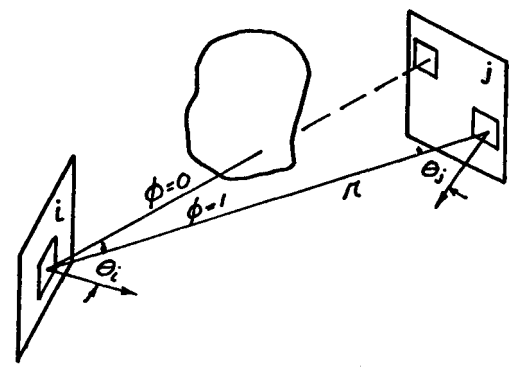

Fig. 3 Radiation between two surfaces with a partially obstructed view.

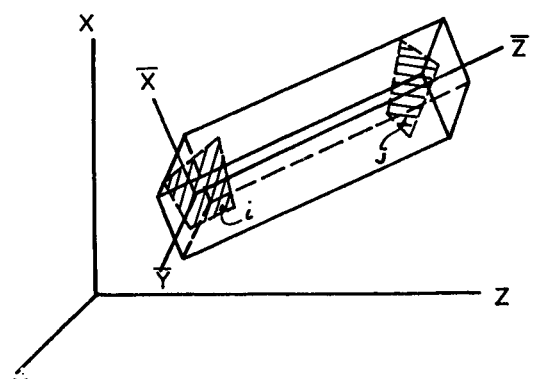

Fig. 4 Redefinition of coordinates to minimize the view prism.

To examine this question, the two problems illustrated in Fig. 5 were treated. The results are given in Tables 1 and 2. Two different models were used: 1) the sector radius was the original circle radius, 2) the radius was adjusted such that the area of each flat surface was equal to the area of the corresponding curved surface.

The results indicate that slightly better results are obtained when the radius is varied. However, at the point where the error is of the order of 1%, either method will suffice. The results indicate that sector angles of the order of 15 deg are sufficient for accurate calculations. Increasing the number of radial divisions yields only a marginal improvement. Of course, if the problem involves an obstruction, an increased number of divisions will improve the obstruction calculations.

The cylinder problem (Fig. 5b) tests both the ability of a flat surface to model a curved surface and the ability of the obstruction solution to treat a case where the obstruction is very severe. In this case, the obstruction occurs because the central cylinder blocks a significant protion of the view that the outer cylinder has of itself and of the annular end surfaces. The dimensions were chosen to ensure that the obstruction effect was large. Table 2 presents the results. In the variable radius case, both cylinder radii were adjusted to preserve the correct surface areas, although this resulted in a slightly incorrect annular area. In contrast to the disk problem, ensuring that the surface area equalled that of the cylinder did not improve the results.

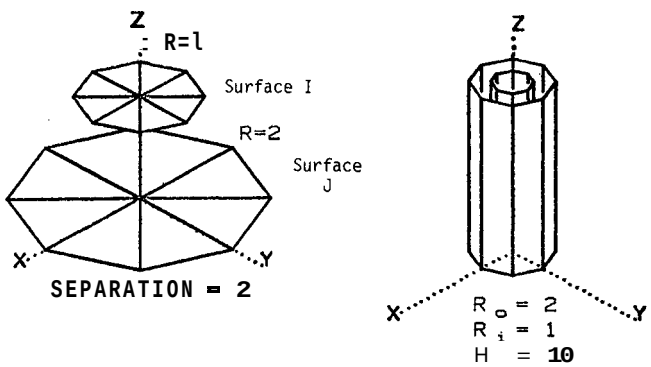

Fig. 5 Radiation between curved surfaces and disks.

Table 1 View factor from surface i to surface j [exact value = 0.46887 (Fig. 5a)]

Radial increments	Sector angle	Constant radius	Variable radius
1	90.0	0.36179	0.46228
1	45.0	0.44430	0.46863
1	22.5	0.46287	0.46887
1	11.25	0.46738	0.46887
1	5.625	0.46849	0.46887
2	90.0	0.36198	0.46228
2	45.0	0.44489	0.46863
2	22.5	0.46401	0.46887
2	11.25	0.46864	0.46887

Table 2 View factors between finite length coaxial cylinders [exact value = 0.92917 (Fig. 5b)]

Sector angle	Constant radius	Variable radius
90.0	1.89576	1.72536
45.0	0.94598	0.94308
22.5	0.94182	0.94120
11.25	0.93062	0.93042
5.625	0.93050	0.93064

A comparison of the disk and cylinder results indicates that it requires fewer subdivisions to model the cylindrical surface by planes than it takes to model the curved boundary of the disk by straight edges. In either case, it appears that to achieve an error on the order of 1%, requires the use of an angular increment in the neighborhood of 15 deg, or approximately **24** lateral flat planes to model a cylinder.

The One-Dimensional Element

Consider the rather simple space frame shown in Fig. 1. Using the results of the previous section, it would be necessary to represent each member by at least eight flat planes (and preferably 24), for a total of 120 surfaces. Based upon previous benchmark timing tests, this would require Something on the order of 1500 s of CPU time on a CDC Cyber 175/750. Obviously such a calculation is not feasible for even the simplest space frames.

Suppose that each rod, or one-dimensional element, is represented by a rectangular plane, Fig. **6,** which rotates to simulate a cylinder according to the following assumptions:

1) This rectangle rotates about the axis of the cylinder such that the maximum area is exposed to the other surfaces. Thus the orientation of the rectangle is different when viewed from each of the other surfaces.

2) For a nonobstructed view, the view factor is computed using contour integration and rotating the rectangle such that the cross-sectional area is maximized when viewed looking from the centroid of surface i to the centroid of the one-dimensional element. This is only accurate when the area of surface i is not large in comparison to other surfaces.

3) When computing the view factor between two surfaces, i and j, whose view is obstructed by a one-dimensional element, the rectangle is rotated to present the maximum cross-sectional area when viewed looking from the centroid of surface i to the centroid of surface j. More accurate calculations would require that this rotation be done for each ray from surface i to j.

The Rectangle as a Representation of the Cylinder

The first question to be resolved is whether a rectangle, equal in size to the plan view of the cylinder, can be used to model the cylinder, and under what conditions the modeling will be accurate. **As** an example, consider two parallel, infinitely long cylinders. The error in computing the view factor by approximating the cylinders by rectangles is shown in

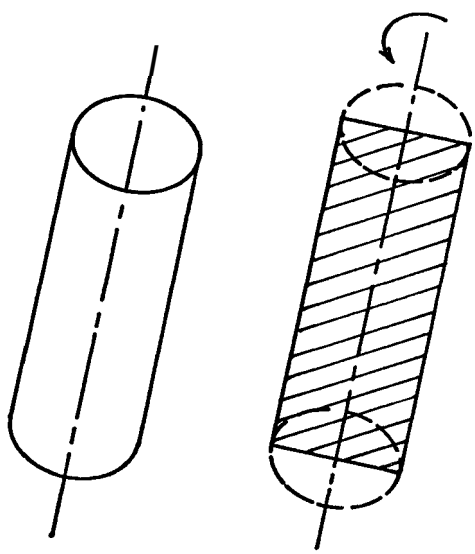

Fig. 6 Modeling a cylinder by a rotating plane.

Fig. 7. For separation distance such that $S/D > 5$, the error is less than 1%. A series of computations for finite length cylinders showed that for length-to-diameter ratios >3 the error is approximately the same as for infinitely long cylinders of the same value of S/D. For cylinders for which $S/D < 5$, or for cylinders close to large flat surfaces, the only sure method is to represent the cylinder by 8-24 flat surfaces. Of course such problems are not, by their very nature, one-dimensional problems.

Rotations for Each Ray

When the axis of a cylindrical surface is directed at another surface, as for example surface 4 of Fig. 1 is directed toward surface S, contour integration is inappropriate, and double-area integration must be used. This requires that the rectangle be rotated for each ray drawn to surface S. Usually the fact that the one-dimensional element is perpendicular, or nearly so, to surface S implies that view factor from surface S to surface 4 is small and it might be thought that ignoring this rotation would suffice. A number of experiments showed that this rotation could not be neglected because 1) although F_{S4} is small, primarily because the area of surface 4 is small, this very smallness of A_4 leads to substantial errors in evaluating F_{4S} by reciprocity since $F_{4S} = A_S * F_{S4}/A_4$; 2) unless the plane is rotated, $\cos\theta_4$ for some of the rays was negative, and the cancellation of positive and negative values of f_{nm} often led to negative values of F_{S4}.

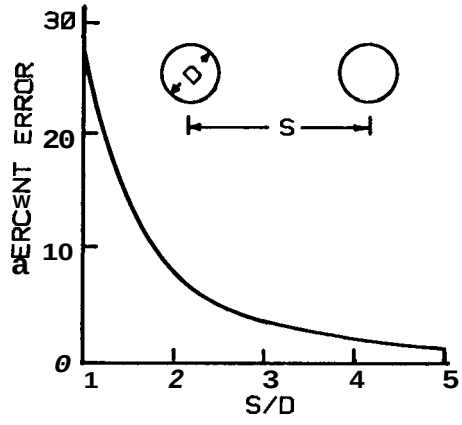

Fig. 7 Error introduced by modeling a cylinder by a rectangle.

Rotations for Obstructions

The next question was how important was it to rotate the rectangle to present the maximum obstruction cross section to each of the rays drawn from one surface to another. With regard to Fig. 1, can the rectangle which represents suface 3 be rotated just once with respect to the line between the centroids of surfaces S and 4, or must it be rotated for each ray between the two surfaces?

To gain some experience using one-dimensional elements to compute obstructed view factors, the problem shown in Fig. 8 was considered. Table 3 lists the results in terms of the separation distance *d*. The "cylindrical" values were computed by assuming that the obstructing cylinder was represented by a series of eight vertical panels. We note that the number of rays obstructed and the view factor $F_{,}$, is the same for both methods. The view factors between the cylinder and other surfaces were found to be about 10% low. These low values of the view factor were due to the closeness of the cylinder to the other surfaces, $S/D = 0.5$, in which case, as discussed previously, the approximation of the cylinder by a flat rectangle underestimates the view factor, Fig. 7.

If a cylindrical surface is represented by only a few rectangular panels, the rotational orientation of the rectangles

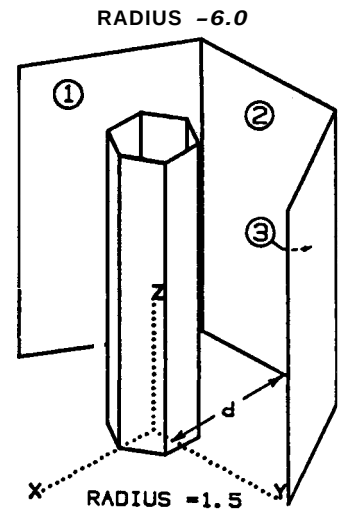

Fig. 8 Schematic of the obstruction calculations used to test the one-dimensional element by considering concentric cylinders.

Table 3 One-dimensional obstruction calculations view factor from surface 1 to surface 3 and from the cylinder to surface 2 (Fig. 8)

Distance,	Surfaces 1 to 3		Cylinder to 2		No. of obstructed rays between 1 and 3	
d	Cvlinder	1-D	Cylinder	1-D	Cvlinder	1-D
3.19	0.04093	0.04093	0.21778	0.18009	208	208
5.19	0.13194	0.13194	0.13705	0.12096	48	48
10.19	0.15235	0.15235	0.05772	0.05478	0	0
15.19	0.15235	0.15235	0.03081	0.03029	0	0
		Rotation = 10 deg				
3.19	0.05063	0.04093	0.23968	0.18009	192	208
5.19	0.13194	0.13194	0.13641	0.12096	48	48
		Rotation = 20 deg				
3.19	0.05063	0.04093	0.23733	0.18009	192	208
5.19	0.13194	0.13194	0.13719	0.12096	48	48
		Rotation = 30 deg				
3.19	0.04841	0.04093	0.23787	0.18009	192	208
5.19	0.13194	0.13194	0.13934	0.12096	48	48

may create errors because of the number of rays obstructed. Table 3 illustrates the effect of rotating the inner cylinder. Preliminary results indicate that sector angles of less than 15 deg are needed to eliminate this orientation effect. The one-dimensional element does not suffer from this problem because the rectangle is automatically rotated to present the largest obstruction between any two surfaces. The results indicate that the rotating rectangle can be used effectively to model an obstructing surface even when the cylinder is too close to the other surfaces to give accurate values for radiation from the cylinder itself to the other surfaces.

Similar tests were made for a variety of different cylinder-pair configurations. Although the errors varied slightly, both in magnitude and shape, the general conclusions cited previously were found to apply for all problems tested.

The one-dimensional element is intended to model a thin cylinder for which $S/D \gg 1$. If $S/D < 1$, then the cylinder should be represented by subdividing the circumference into a number of rectangular panels. Under some conditions, such as near the confluence of the legs of a tripod, a cylinder will satisfy $S/D \gg 1$ at some points along its length, while at other points, $S/D < 1$. A decision to model such a tripod leg by a single one-dimensional element or by a combination of one-dimensional and cylindrical elements depends upon the importance attached to the radiation heat transfer near the juncture.

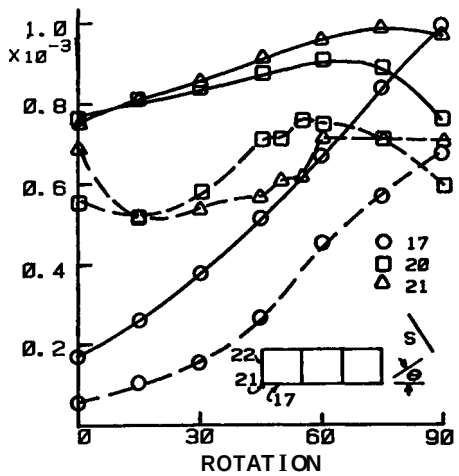

Fig. 9 View factors from surface S to surfaces 17, 20, and 21 (Fig. 1): ——unobstructed view (i.e., no other frame members), — — obstructed view.

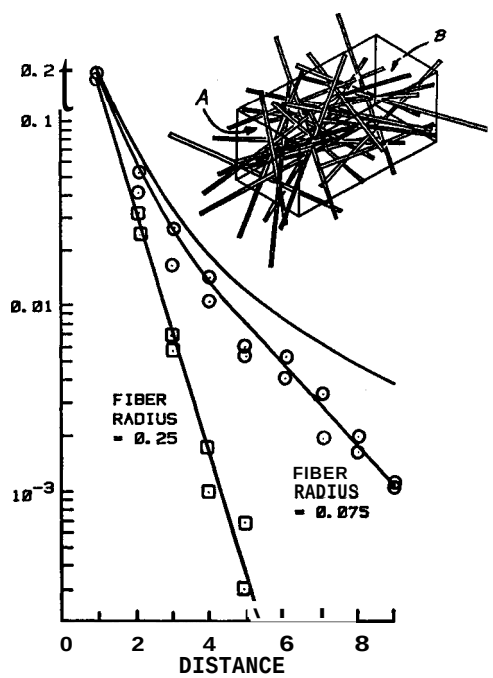

Fig. 10 Direct view factor through fibrous insulation from surface A to surface B.

Examples of the Use of the One-Dimensional Element

The Space Frame

The radiation from surface S, Fig. 1, to several of the frame members was computed as a function of the position of surface S. Before discussing these results, it is of interest to examine the question of the effect of the number of rays used in the calculation and the possibility that, because of the finite number of rays, the number of obstructed rays will change quite discontinuously as surface S is moved and the results may be significantly in error. Table 4 lists the number of rays blocked and the computed view factors as surface S (located at $x = -15$) was moved either vertically or horizontally.

Because of the small diameter of the cylinders and the large spacing of the surfaces, it is not expected that the view factor will change appreciably with position. As shown in Table 4, there is a small change in the value of F_{S4} even if surfaces 1, 2, and 3 are not present because of the changing values of $\cos\theta_S$ and $\cos\theta_4$. The effect of the blockage of rays to reduce the view factors is quite evident. Computations performed with different number of rays did not yield substantially different results.

Figure 9 illustrates the changes in the view factors as surface S rotates around the space frame as shown in the inset. The on-off blocking characteristics of the frame members as surface S moves about the frame are clearly evident. This is particularly true for element 21, whose radiation is blocked by all of the triangular legs until surface S is rotated sufficiently such that it is above surfaces 2 and 3 (i.e., 50 deg). From this point onward, the blockage is nearly constant since only the portion near the apex of each triangle serves to obscure the view and the end surfaces (surfaces 17-22) are finally getting a relatively clear view of surface S. The small irregularities in the values for surfaces 20 and 21 are due to the discontinuous blocking of the finite number of rays. This effect can be reduced only by increasing the number of rays.

Table 4 Effect of the movement of surface S on the value of F_{S4} (16 rays per surface)

Position of centroid of S		Fs4		
		Considering surface 4 only	Considering surfaces 1-4	
Y	Z	(no blockaee)	(blockage)	Rays blocked. %
0.0	2.0	0.002270	0.001249	21.9
	2.5	0.002235	0.001190	28.1
	3.0	0.002191	0.001370	34.4
	3.5	0.002139	0.001153	37.5
	4.0	0.002082	0.001106	37.5
	4.5	0.002024	0.001033	34.4
	5.0	0.001970	0.000987	40.6
	5.5	0.001927	0.001166	40.6
	6.0	0.001888	0.001014	40.6
	6.5	0.001854	0.000993	40.6
	7.0	0.001824	0.001037	34.4
	7.5	0.001804	0.001307	40.6
	8.0	0.001793	0.001344	37.5
−0.5	5.0	0.001698	0.001034	39.1
−1.0		0.001966	0.001059	39.1
−1.5		0.001978	0.001125	35.9
−2.0		0.002005	0.001230	32.8
−2.5		0.002029	0.001221	31.2
−3.0		0.002051	0.001320	29.7

However, the results shown in Fig. 9 are sufficiently smooth for most computations. The computation for a single position of S requires 6 s of CPU time on the CDC Cyber 175/750, illustrating the efficiency of the use of the rotating plane to model the rod. This compares with a time of 1500 s if eight planes were used to model each rod.

Fibrous Insulation

A rather intriguing application of the one-dimensional element is in the computation of the extinction coefficient for the fibrous insulation shown in Fig. 2, which was taken as a model of the expanded silica insulation used in the Space Shuttle tiles, In such a medium, the radiation is affected by scattering, specular and diffuse, and refraction. Tong and Tien[8] have presented an analytical development for radiation in the presence of multiple scatterers found in typical insulations, and Cunnington et al.[9] have applied their results to composite fibrous systems whose fiber sizes are somewhat equivalent to the tile material.

The Shuttle tiles are made of silica fibers, whose diameters range from 1.5 to 3 pm. Since the case of greatest interest is when the tile surface is hottest (1500 K), the dominant radiative wavelength will be on the order of 2 μm, leading to Mie scattering from the fibers. Due to the type of scattering, the method described herein is not appropriate to the original type of tile material. The newer, fiber-reinforced tile, FRCI,[10] contains randomly located fibers of AB312 (aluminum borate) whose diameters are on the order of 10-20 μm and whose surfaces have imperfections on the order of 0.1 μm.[9,10] Under these conditions, these larger fibers appear to be large ($D/\lambda \geq 5$) and diffuse and their effect on short-wave radiation may be computed by the method described herein.

In the model, the fibers were contained in a rectangular parallelpiped $3 \times 3 \times 10$ units located by defining their centroids and the angles the fibers made with the x-y and x-z planes. The coordinates of the centroids and angles were chosen on the basis of random number distributions such that the fiber density was constant, increased linearly, or decreased linearly with respect to x.

The radiation passing through the insulation was computed by determining the view factor between surface A located at the left edge of the prism and a similar surface, B, placed within the prism at different distances from surface A. Figure 10 displays the view factor for different separation distances and two fiber diameters. Two different calculations were made. In the first, surface A was located at $x = 0$ and surface B was moved from $x = 1$ to 10. In the second, surface A was located at $x = 10$ and surface B was moved from $x = 9$ to 0. In this way, the results give some idea of the variation to be expected at different positions within the insulation due to the random distribution of fibers. The vertical scatter shown on Fig. 10 is due to this random distribution.

Note that the view factors decrease semilogarithmically only after an initial nonlinear decay. The early nonlinear part of the reduction of the view factor is due primarily to the rapid reduction in solid angle subtended by surface B. The later, semilogarithmical reduction is associated primarily with the blockage of the radiation by the fibers. The effect of the ray blockage is clearly seen by comparison to the curve for no blockage. Note that, in general, the greater the extinction, or the less the view factor, the less scatter due to the fiber blockage since the separation distance is such that nearly complete obstruction has occurred. The greater obstruction cross-sectional area of the large-diameter fibers also gives rise to the semilogarithmic behavior at shorter separations than the less obstructing smaller diameter fibers.

The results for the nonuniform variation of fiber density were substantially different than the semilogarithmic variation found for the uniform case and did not lead to the determination of an effective extinction coefficient.

Although a simplistic idea, if one assumes that for a low density of fibers all scattered rays are reflected out of the parallelepiped, then the blockage of transmitted radiation can be directly related to the radiative scattering. Assuming a fiber diameter of 10 pm, and computing the extinction due to ray interception, the ratio of the extinction coefficient to the volume fraction is on the order of 10^5 for the small fiber case. This value is in good agreement with the scattering coefficient reported by Tong and Tien.[8]

This example shows that the one-dimensional radiation element can be used successfully and efficiently for the analysis of complex structures, typical of the space frames expected to be utilized in space systems. In related computations, we have found that it is an effective method for computing the solar radiation transmitted within such structures.

Conclusions

The use of a rotating rectangle to model a one-dimensional radiation element is shown to be both computationally efficient and accurate. Because of the reduced computational cost of this element, radiation view factors for complex structures are amenable to direct calculations. Under some conditions, the very nature of the one-dimensional element may lead to a loss in accuracy when it is used to model obstructing cylinders. In these cases, in which the element is too close to the radiating surfaces, curved surfaces must be represented by a collection of flat planes. However, it appears that as long as the one-dimensional element is more than 5 diameters from the other surfaces, its use is valid.

Acknowledgments

This work was conducted under the auspices of the National Aeronautics and Space Administration, Grant NAG-1-41. The authors wish to express their appreciation to the contract monitors A. Wieting and C. Pittman.

References

'Sparrow, E. M. and Cess, R. D., ***Radiation Heat Transfer,*** Brooks/Cole Publishing Co., Belmont, Calif., 1966.

[2]Hottel, H. C. and Sarofim, A. F., ***Radiative Transfer,*** McGraw-Hill Book Co., New York, 1967.

[3]Siegel, R. and Howell, J. R., ***Thermal Radiation Heat Transfer,*** McGraw-Hill Book Co., New York, 1972.

[4]Howell, J. R., ***A Catalog of Radiation Configuration Factors,*** McGraw-Hill Book Co., New York, 1982.

[5]Emery, A. F., Kippenhan, C. J., Mortazavi, H. R., and Wieting, A. R., "Computation of Radiation View Factors for Surfaces with Obstructed Views of Each Other," ASME Paper 81-HT-57, Milwaukee, Wis., 1981.

[6]Emery, A. F., Mortazavi, H. R., and Kippenhan, C. J., "Interactive Computation of Radiation View Factors," NASA CP 2216, 1982, pp. 221-242.

[7]Emery, A. F., Mortazavi, H. R., and Nguyen, M. N., "The Numerical Computation of Diffuse Radiation in Complex Structures Filled with a Semi-Transparent Medium," ***Proceedings of the Third International Conference on Numerical Methods in Thermal Problems,*** Seattle, Wash., Aug. 1983.

[8]Tong, T. W. and Tien, C. L., "Radiative Heat Transfer in Fibrous Insulations," ***ASME Journal on Heat Transfer,*** Feb. 1983, pp. 70-81.

'Cunnington, G., Wedel, R., and Thomas, J., "Radiation in Composite Fibrous Media," AIAA Paper 84-1791, 1984.

[10]Mueller, J. I. and Bollard, R. J. H., "Special Status Report, No. 3," NASA-NSG 48-002-005, Dec. 1981.